The Fluxus-1 and -2 active experiments: Investigation of plasma jet dynamics and interactions with the ionosphere

J. I. Zetzer[1], B. G. Gavrilov[1], Yu. N. Kiselev[1], V. A. Rybakov[1], V. Gritskiv[2], Yu. A. Romanovsky[3], R. E. Erlandson[4], C.-I. Meng[4], and B. J. Stoyanov[4]

Abstract. This paper presents an overview of two Russian-American active geophysical rocket experiments, Fluxus-1 and Fluxus-2, designed to study the interaction of plasma jets with the ionosphere and magnetosphere. These active experiments used specially designed explosive type shaped-charge generator (ETG) that produces a 3-MJ aluminum plasma jet without the aid of solar illumination. The jet was injected nearly parallel to the magnetic field at an altitude of 140 km towards an instrumented payload located 130 m away. The plasma jet density exceeded 1×10^9 ions/cm^{-3} and produced over a 50% reduction in magnetic field strength due to a diamagnetic depression. The experiment was also observed using ground-based visible sensors, and space-based ultraviolet, visible, and infrared sensors on the Midcourse Space Experiment (MSX). It was found that the plasma jet was quickly stopped due to collisions with the atmosphere and formed a slowing moving (100 m/s) plasma cloud that was observed for up to 3 minutes using visible sensors.

1. Introduction

The Fluxus-1 and Fluxus-2 experiments were launched using MR-12 meteorological rockets from Kapustin Yar, Russia, as part of a joint Russian-American program to study the interaction of a high-speed artificial plasma jet with the neutral atmosphere, ionosphere, and magnetosphere.

The Fluxus experiments differ from previous active rocket experiments [Kozlov and Smirnova, 1993] in that the Fluxus shaped-charge device produces a high-speed plasma jet in the absence of solar illumination. In addition, the plasma jet has been calibrated, allowing the device to be used as a controlled device to perturb the ionosphere.

This calibrated source, referred to as an explosive type generator (ETG), was developed to create a high-speed plasma jet of known composition [Adushkin et al., 1993]. This ETG, designed to create a plasma jet in the absence of solar illumination, allows one to study the ionization, recombination, and interactions of the jet with the atmosphere and ionosphere. In this way, the effects due to the environment interactions can be separated from those associated with solar illumination effects. Furthermore, the capability to generate a high-speed plasma jet at night allows weak optical emissions associated with the jet to be observed.

2. Instrumentation

During the Fluxus-1 and -2 experiments, the plasma jets were injected into the early morning sector (~0500 LT) mid-latitude (dip latitude = 65°) ionosphere near apogee at an altitude of 140 km. The plasma jet experiments took place on January 31, 1997, at 0201:46 UT and on February 5, 1997, at 0218:43 UT. Geophysical conditions were relatively quiet during both experiments. The *Kp* index was 3 and 1 for Fluxus-1 and -2, respectively.

The payload consisted of an instrument and ETG payload. These payloads were separated by 130 m when the ETG detonated. The orientation of the payloads and plasma jet with respect to the local geomagnetic field is shown in Figure 1. The relative orientation and distance between the ETG and the instrument payload in Figure 1 is based on nominal values and data collected by a magnetometer on the instrument payload.

The instrument payload contained sensors designed to observe the plasma jet and interactions of the jet with the ionosphere. A list of sensors on this payload is given in Table 1. The electric field receiver, Langmuir probes, and three-axis magnetometers were placed on fold-down booms. The ion traps, low-energy electron detectors, Geiger counters, pyroelectric sensors, and visible photometers were placed on the front face of the payload facing the direction of the ETG payload.

The ETG payload contained the ETG, initiator, and radio-frequency beacon used by the MSX satellite beacon receiver to track (point at) the ETG payload experiment.

The ETG produces a calibrated aluminum high-speed plasma jet. This jet is formed using high-power explosives that vaporize a solid porous working substance (aluminum) and accelerate these vapors by a converging shock wave (Figure 2). The Al is ionized by this shock wave. The total weight of the explosive was 4.9 kg and working substance was 22 g. This represents a total explosive energy of 20 MJ and produces a plasma jet with a total energy of 3 MJ.

The source was calibrated on the ground by using sub-scale models of the ETG. It was found that 92% of the plasma jet mass and energy is concentrated within 20° of the jet axis. The velocity distribution of the 22-g plasma jet was such that 10 g exceeded 10 km/s, 3 g exceeded 25 km/s, and 0.01 g exceeded 40 km/s. The plasma jet energy is 3 MJ.

[1] Institute for Dynamics of Geospheres, Moscow, Russia
[2] NPO Typhoon, Moscow, Russia,
[3] Institute of Applied Geophysics, Moscow, Russia
[4] The Johns Hopkins University Applied Physics Laboratory, Johns Hopkins Road, Laurel, MD 20723

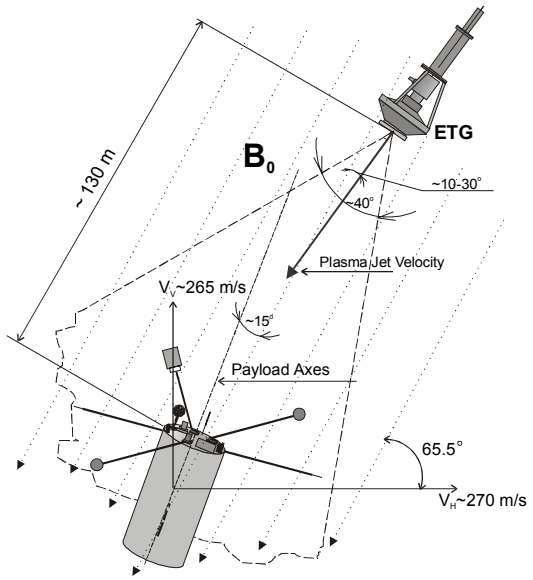

Figure 1. Orientation of the plasma jet and payload with respect to the geomagnetic field.

The jet brightness temperature was 16,000 K and <5,300 K at distances from the exit orifice of 10 and 30 cm, respectively. The plasma jet was sharply terminated 27 μs after the detonation in order to cut off debris associated with the explosion, resulting in a minimum plasma jet speed of 7 km/s.

The experiment was coordinated with the MSX satellite. A radio-frequency transmitter was placed on the ETG payload so that MSX could point at the ETG payload during the plasma jet event [Mill et al., 1994]. MSX acquired data from the far ultraviolet (113 nm) through the very long wave infrared (28 μm) [Mill et al., 1994]. MSX spectral observations of the Fluxus-1 and 2 experiments in the visible and ultraviolet are reported in this issue by Erlandson et al. [1999]. A number of sensors were also placed at different sites on the ground and on an airplane. These sensors included low-light level visible cameras and a high-speed photometer that was sampled at a rate of 10 kHz.

3. Observations

The time history of visible emissions collected using a ground based photometer and camera is shown in Figure 3. The evolution of the plasma jet was sub-divided into three stages based on the data shown in Figure 3. The three stages occur at times of 0 – 0.001 s, 0.001 – 0.05 s, and 0.05 – 180 s.

In the first stage (t < 0.5 ms) the jet traveled a distance less than one mean free path. This represents free expansion of the jet in the absence of collisions with the neutral atmosphere. The first peak observed using the ground-based photometer, sensitive from 350-650 nm, is observed during this first stage, 0.3 ms after the ETG. Optical emissions were also recorded using a visible (40-500 nm) and near-infrared (1300-1600 nm) photometer on the instrument payload. These photometers were sampled at a higher rate (100 kHz) than the ground based photometers and recorded a more complex intensity profile during the first stage of plasma jet expansion (Figure 4). The instrument payload photometer each recorded two peaks in intensity during the first stage (t < 0.5 ms), where the near infrared band lags the visible band. Both of these peaks were observed prior to the arrival of the jet at the instrument payload [Gavrilov et al., 1999]. The radiation temperature reached a maximum value of 9000 K during the first peak, 20 μs after the ETG detonation. In subsequent intensity peaks (t>1x10-4s), the jet was not in equilibrium.

The second stage of the plasma jet expansion lasted from 0.00l to 0.05 s. In this stage, the jet had already traveled farther than one mean free path and thus had begun to interact with the atmosphere. This is the stage resulting in the strongest radiation. The radiation is greater in the visible than in the infrared (Figure 4). The ratio of the blue to red bands indicates that the jet is in a strongly non-thermal equilibrium state during this stage.

The third stage of the plasma jet evolution lasted from 0.05 to at least 180 s (180s was the end of the

Instruments	Band or Sensor Type	Range	Sampling Rate
Photometers	400–500 nm and 1.3-1.6 μm	5×10^{-6} to 1×10^{-3} W	10^5 Hz
Pyroelectric sensor	10–4000 nm	10^{-4}–10^{-6} J/cm^2	10^4 Hz
Pyroelectric sensor	200–4000 nm	10^{-6}–10^{-3} W/cm^2	10^5 Hz
Magnetometer		500–50,000 nT	5×10^4 Hz
Langmuir probe	Cylindrical probe, Fixed Bias	10^6–5x10^9 cm^{-3}	10^5 Hz
Langmuir probe	Cylindrical probe, Fixed Bias	10^6–5x10^9 cm^{-3}	10^5 Hz
Langmuir probe	Cylindrical probe, Fixed Bias	10^4–10^6 cm^{-3}	10^4 Hz
Spherical ion trap		10^3–10^6 cm^{-3}	100 Hz
Flat ion trap		10^3–10^6 cm^{-3}	100 Hz
Electric fields	dc	1–1000 mV/m (dc)	0–20 Hz (dc)
	ac	5×10^7 V/mHz$^{-1/2}$ (ac)	0.02–20 kHz (ac)
Geiger counter	> 40 keV		500 Hz
Electron detectors	0.3 and 1.0 keV	10^5–10^8 e^-/(cm^2 sr s keV)	500 Hz

Table 1. Instrument payload sensors.

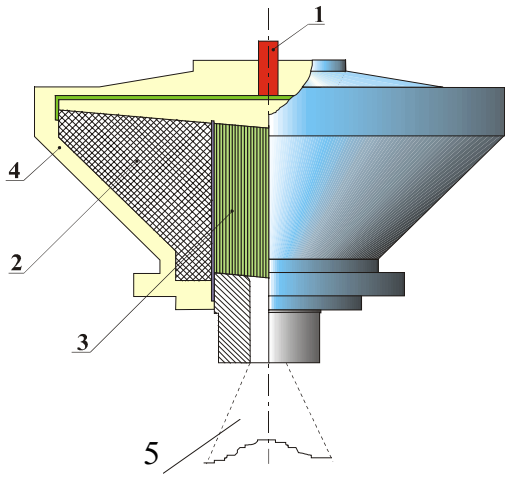

Figure 2. ETG design. The components consist of the initiator (1), explosive (2), solid body (3), structure (4), and plasma jet (5).

ground-based camera data taking interval). In this stage, the high-speed plasma jet evolves into a slowly moving luminous region that more closely resembles a cloud rather than a jet. Therefore, in this luminous region is referred to as a plasma cloud. The intensity of the plasma cloud reaches a maximum 100 s after the plasma jet injection (Figure 3). The cloud expands to a diameter of 2 km in the first 10 s and then expands more slowly during the next 170 s to a diameter of 4 km. The expansion of the cloud is controlled by the diffusion of the cloud in the ambient atmosphere, although the more rapid expansion during the first 10s is not presently understood.

Photochemical processes in the atmosphere, most likely drive the third stage or plasma cloud stage. Spectral features associated with the cloud were not observed in the data collected by the MSX ultraviolet and visible spectrographic imaging sensors. This is most likely due to the fact that the source of the visible plasma cloud is due to reactions of AlO with H_2O forming HALOH. Ground-based visible imagery was used to determine that the cloud drifted at a relatively constant speed of 100 m/s to the south during the third stage. The total amount of energy radiated by the plasma jet/cloud during the third stage was around 500 kJ. This represents ~20% of the total jet energy and significantly exceeds the amount of energy radiated in the other two stages.

The three-axis magnetometer on the instrument payload, located 100 m from the ETG payload, recorded a substantial reduction in the magnetic field from 3 to 30 ms after the plasma jet injection. The magnetic field intensity decreased from about 0.5 to 0.2 G, consistent with magnetic field expulsion by the high-density plasma jet whose density is estimated between 10^9 and 10^{10} cm^{-3} [Gavrilov et al., 1999].

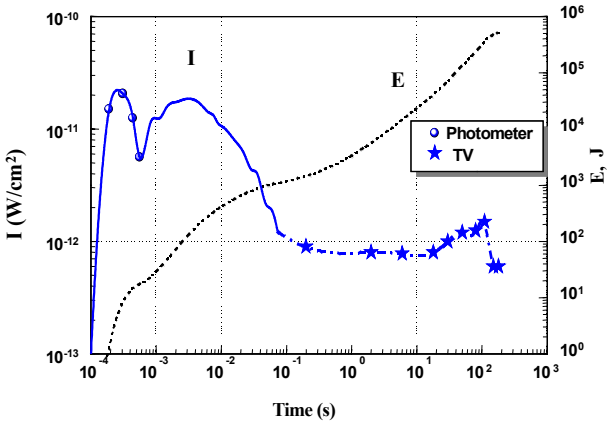

Figure 3. Irradiance from the plasma cloud (in a bandwidth 350–650 nm) on a surface of the Earth and the total radiated energy.

Electric field enhancements were also associated with the plasma jet. The maximum amplitudes were 300 mV/m and 450 mV/m during Fluxus-1 and -2, respectively. An unexpected feature in the Fluxus experiments was the periodic nature of these pulses. During Fluxus-1, three electric field pulses separated by 0.5 and 0.3 s were observed (Figure 5). These enhancements may be due to an Alfvén wave that excites the ionospheric Alfvén resonator, causing a pulsation in the electric field [Poliakov and Rapoport, 1981; Lysak, 1993].

The flux of electrons at 0.3 and 1.0 keV increased by a factor of 40–50 during the plasma jet experiment. These electrons may be associated with the jet or ambient electrons involved in the jet neutralization. There was no change in the flux of high energy (>40-keV) electrons during the experiment

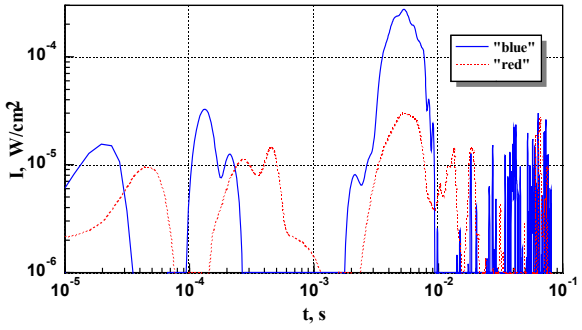

Figure 4. High time resolution optical emissions of the Fluxus-1 plasma jet using on-board blue (400–500 nm) and red (1300–1600 nm) photometers.

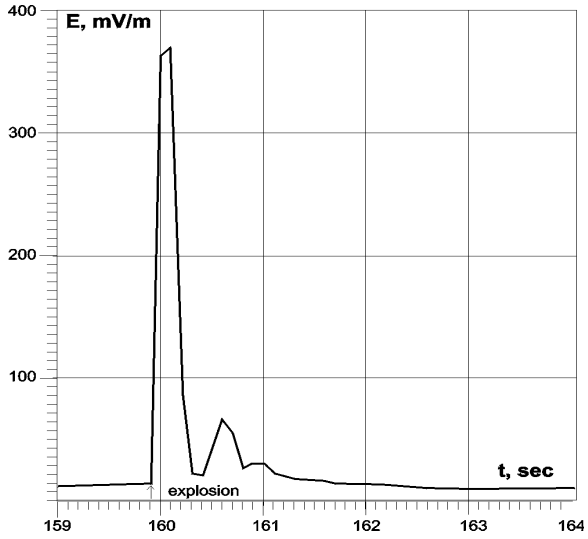

Figure 5. Quasi-static electric field intensity recorded by the electric field instrument during Fluxus-1.

The response of the ionosphere was also measured during the experiment. This was done using an inclined Doppler sounding method at frequencies of 5795–9625 MHz. Radio receivers on the ground which measured waves reflected from the ionosphere at distances of 30 and 210 km from the plasma jet injection site showed evidence of wave-like ionospheric disturbances. This is most likely caused by the generation of acoustic gravity waves.

4. Conclusion

The Fluxus-1 and -2 experiments have produced a number of new results on the interaction of high-speed plasma jets with the atmosphere and ionosphere. First, detailed observations of a large-scale diamagnetic depression associated with the high-density jet was observed [Gavrilov et al., 1999]. Second, the plasma jet was found to induce quasi-static periodic disturbances in the electric field as well as an enhanced flux of electrons presumably associated with neutralization of the plasma jet. Third, optical observations of the plasma jet and long-lasting plasma cloud were acquired using sensors on the instrument payload, ground and MSX satellite. During early times ($t < 0.001$ s) the plasma jet radiation suggest radiation temperatures of ~9000K while later in the expansion ($0.001 < t < 0.05$ s) the radiation was not in thermal equilibrium. Spectrographic imagers on MSX observed emission features were associated with Al^+, Al, AlO, and enhancements in terrestrial airglow emissions such at 135.6 nm and 557.7 nm [Erlandson et al., 1999]. During the third stage of the plasma jet expansion, the jet formed a luminous plasma cloud that was observed for 180s. The long lifetime of this cloud was not expected. The intensity of the cloud was too weak to be observed using the MSX spectrographic imagers. It is speculated that the source of the long-lasting cloud are emissions due to HAlOH (A – X) formed by the reaction of Al dimers, atomic oxygen, and water vapor.

Acknowledgments. The authors thank the sponsors of these experiments and all the colleagues who participated in the experiment preparation, operations, and analysis.

References

Adushkin, V. V., J. I. Zetzer, Yu. N. Kiselev, I. V. Nenchinov, and B. D. Christoforov, Active geophysical rocket experiments in the ionosphere with the high velocity plasma jet injection, *Doclady RAS, 331*(4), 486–489, 1993.

Erlandson, R. E., P. K. Swaminathan, C.-I. Meng, B. J. Stoyanov, J. I. Zetzer, B. G. Gavrilov, Yu. N. Kiselev, and Yu. A. Romanovsky, Ultraviolet-visible imagery and spectra of the Fluxus-1 and -2 artificial plasma jet, *Geophys. Res. Lett*., submitted, 1999.

Gavrilov, B. G., A. I Podgorny, I. M. Podgorny, D. B. Sobyanin, J. I. Zetzer, R. E. Erlandson, C.-I. Meng, and B. J. Stoyanov, Diamagnetic effect produced by the Fluxus-1 and -2 artificial plasma jet, *Geophys. Res. Lett*., in press, 1999.

Kozlov, S. I., and N. V. Smirnova, Techniques and means of creating artificial formations in the upper atmosphere: Analysis of characteristics of artificial disturbances, *Cosmic Res., 30*, 402–425, 1993.

Lysak, R. L., Generalized model of the ionospheric Alfvén resonator, in *Auroral Plasma Dynamics*, edited by R. L. Lysak, AGU Monograph 80, p. 121, 1993.

Mill, J. D., et al., Midcourse Space Experiment: Introduction to the spacecraft, instruments and scientific objectives. *J. Spacecr. Rockets, 31*(5), 900–907, 1994.

Oraevsky, V. N., Yu. Ya. Ruzhin, V. S. Skomarovsky, V. G. Korobeinikov, A. I. Kashrih, and V. I. Khryukin, Modeling of artificial plasma "bubble" in ionosphere, *Adv. Space Res., 12*(12), 105–107, 1992.

Poliakov, S. V., and V. O. Rapoport, The Alfvén ionosphere resonator, *Geomagnetism and Aeronomy, 21*, 816, 1981.

J. I. Zetzer, et al., Institute for Dynamics of Geospheres, 38, build. 6, Leninsky Ave., Moscow, 117939, Russia. (e-mail: zetzer@idg.chph.ras.ru)

V. Gritskiv, NPO Typhoon, 82 prospect Lenina, Obninsk, Russia, 249020.

Yu. A. Romanovsky, Institute of Applied Geophysics, 9 Rostokinskaya, Moscow, Russia, 129226.

R. A. Erlandson, et al., JHU/APL, Laurel, Maryland, USA. (e-mail: erlandson@jhuapl.edu)